Global stochastic inversion for characterization of a potential subsampled hydrocarbon reservoir

Application of Gassmann´s equation for fluid substitution to calculate the acoustic impedances distributions

Pereira, André Ferreira; Soares, Amílcar; Nunes, Rúben
Email addresses: andre.ferreira.bp@gmail.com; asoares@ist.utl.pt; nunesrfm@gmail.com
Centre for Petroleum Reservoir Modelling
Instituto Superior Técnico
Avenida Rovisco Pais, 1
1049-001 Lisboa

Abstract - The present study applies an innovative methodology that addresses the theme of subsampled fields, intended to generate 3D images of the acoustic impedance (AI) and respective synthetic seismogram. For this purpose was used the global stochastic inversion algorithm for seismic zones (GSI zones), developed by the CERENA team (IST). The definition of the zones model resulted from interpretation of main seismic units, whereas AI local distributions were calculated using the theory of Gassmann fluid substitution. The results allowed to validate the robustness of the algorithm as a viable tool in an early stage of morphological characterization of subsampled hydrocarbon reservoirs by providing relevant and consistent information.

Keywords: Global stochastic inversion, subsampled hydrocarbon reservoirs, Gassmann´s equations for fluid substitution, turbidite depositional systems and reservoirs.

1. Introduction

This thesis results from the need to obtain morphological information to characterize, in the early stages, potential subsampled reservoirs. Reservoir characterization is the most important phase of the entire study process, and provides the decision-making along the production process.

This work applies a methodology that addresses the theme of subsampled fields, designed to generate 3D images of AI and corresponding synthetic seismogram. The benefit in characterize the petrophysical property AI, through global stochastic inversion (GSI) is related to its easy comprehension and its correlation with porosity, which is an important property for evaluating the quality of reservoirs.

The data set used in the study has been provided by Partex Oil and Gas, including a 3D seismic cube in time (soft data), acquired in the deep offshore waters, and logs (transit time - DT and density - RHOB) of three exploratory wells, (W1, W2, W3) (hard data), located on the periphery of the study area (Figure 1).

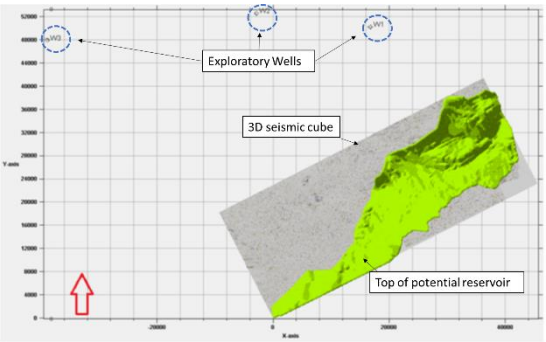

Figure 1 - Study area, with 3D seismic data and three exploratory wells

The seismic volume corresponds to an area of approximately 1040km^2 (52km x 20km). The seismic data acquisition occurred in water depths ranging from 500m to 1150m. The information present on the seismic cube is limited vertically at TWT 2000ms (Figure 2).

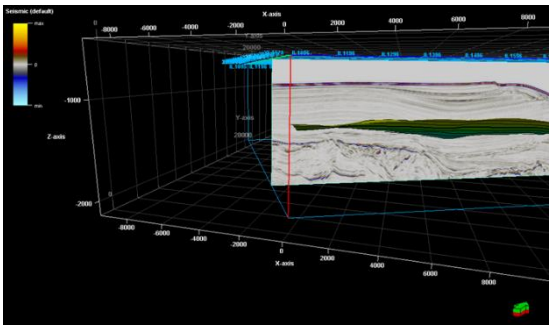

Figure 2 – 3D Seismic cube (Petrel 2013)

The set limit encompasses the seismic units of most interest to this study, the turbidite channels system, dating from the Upper Miocene (Messinian 7-8Ma).

To characterize and evaluate the spatial uncertainty of petrophysical property AI, it was applied an innovative method of GSI, the seismic zones algorithm (GSI zones), developed by CERENA team (IST).

The GSI zones algorithm allowed to combine the geological knowledge of the region under study with the available data, 3D seismic data and logs. The algorithm basis is the creation of a zones model, differentiated by the signatures of seismic reflectors corresponding to different types of lithofacies. To define AI local distributions, for each zone, was used Gassmann´s fluid substitution theory. Two scenarios were defined for the "target" zone, differentiated by the type of simulated fluid (gas or brine). The variogram study was performed for each zone based on the continuity of seismic reflectors.

2. Seismic interpretation and model zoning

The interpretation of the seismic cube, characterization and identification of potential hydrocarbon reservoirs used Petrel 2013 software.

The interpretation of the 3D seismic cube allowed a better understanding of the spatial continuity for the seismic unit target (turbidite channels of the Upper Miocene) and definition of relevant seismic sequences.

The correct definition of several seismic units had fundamental importance in the setting of the seismic zones cube, which served as an input for computing the GSI algorithm.

As part of this work it was necessary to characterize the Mega seismic sequence that includes the seismic unit where the "target" zone is located (defined in the literature as Mega seismic sequence III). Mega seismic sequence III is composed by Neogenic deposits and is limited at the bottom by discontinuity M and at the top by seabed (Figure 3).

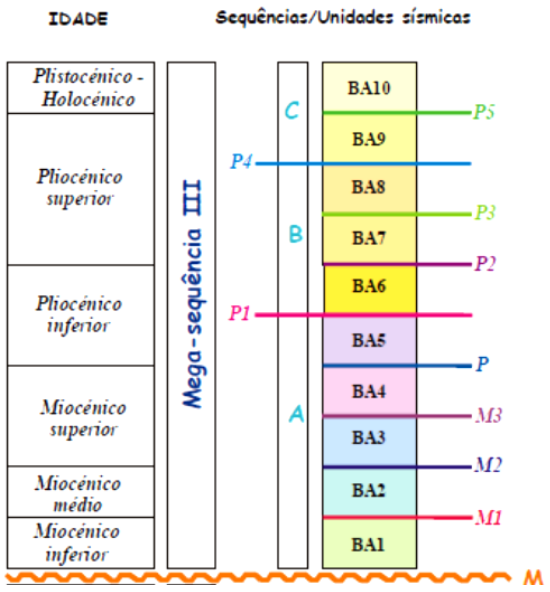

Figure 3 - Stratigraphic column sedimentary basin under study. Roque (2007)

In this Mega sequence it is possible to identify three seismic sequences from the oldest to the newest A, B and C, respectively corresponding to three depositional sequences. These sequences were controlled by different episodes of Neogenic subsidence, which witnesses the occurrence of distinct stages of sedimentary subsidence in the basin.

The three seismic sequences are structured by ten seismic units, designated BA1 to BA10 (Figure 3). The seismic units BA3 to BA5 define the three zones of the seismic cube used in the computation of the GSI algorithm (Figure 4).

This document only describes, in greater detail, the seismic unit BA4 where is located the "target" zone.

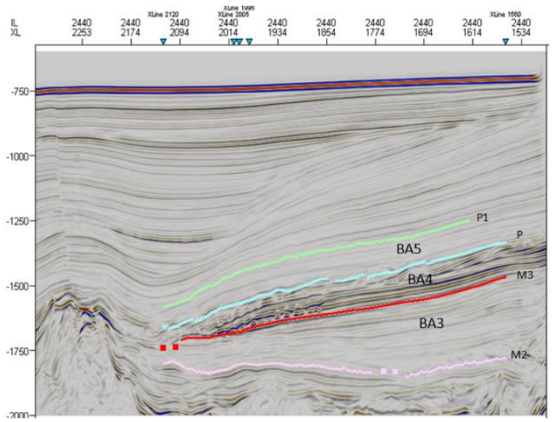

Figure 4 - Interpretation of Inline 2440 (Petrel), with seismic horizons (M2, M3, P and P1) which define the relevant seismic units (BA3, BA4 and BA5) for the case study

The seismic unit BA4 is limited at the base by M3 discontinuity and at the top by P discontinuity, and corresponds to the upper Miocene deposits with approximately 7.0Ma (Figure 5).

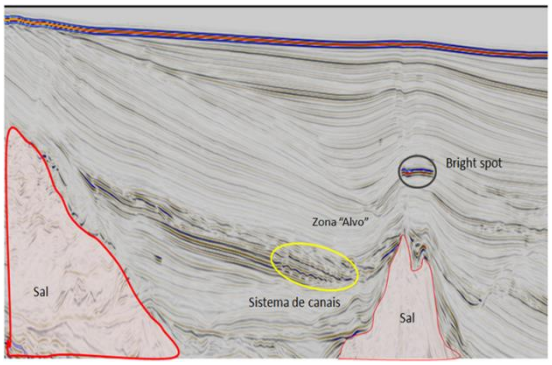

Figure 5 - Petrel view of the original seismic cube (Inline 2507), identification of turbidite channel system - "target" zone and amplitude anomaly "Bright spot"

This seismic unit stands out from the adjacent units for its characteristic stratified parallel facies with internal strong amplitude reflections with high to average continuity. Given the displayed facies it suggests a presence of an extensive sand body of Messinian age (Figure 6).

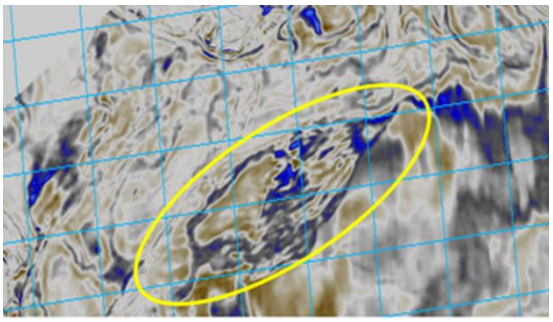

Figure 6 - Original seismic cube "flattened" with the identification of the channel system - zone "target" at TWT 1500ms

According to geological studies of the sedimentary basin, these sands represent depositional lobes of "lower fans" system. This unit consists of clays and silts interbedded with very fine sand lenticles.

The construction of the seismic cube was held in Petrel 2013 software (Figure 7) using the creation of a "simple grid". The model geometry was based on the interpreted seismic horizons, which define the seismic units BA3, BA4 and BA5. The seismic cube scales 235 inlines, 260 crosslines and 600ms vertically. The transformation of seismic amplitudes for the vertical scale is 2ms. The seismic cube has 234x259x300 cells with dimensions 1x1x1. The total area sums 4.368m by 3.225m (14.000km^2). The estimated depth for this potential reservoir is approximately 2.000m, assuming that the average propagation of seismic waves from the ocean bottom to the top of the potential reservoir is 3.500m/s.

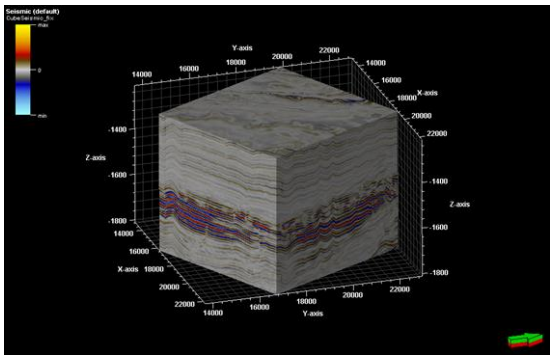

Figure 7 – Seismic cube of amplitudes after grid "regularization"

The model definition with 4 zones (0 to 3) was based on the seismic units BA3 to BA5 as presented in Table 1.

Table 1 – Model zones correspondence used in GSI zones algorithm

Modelo de Zonas				
Zona	**Unidade Sísmica**	**Época**	**Idade**	**Cor**
Zona 0	N/A	N/A	N/A	Roxa
Zona 1	BA5	Pliocénico inferior	Zancleano	Azul
Zona 2	BA4	Miocénico superior	Messiniano	Verde
Zona 3	BA3		Tortoniano	Vermelho

The respective model zones cube, used in GSI zones algorithm, is illustrated in Figure 8 (Petrel view).

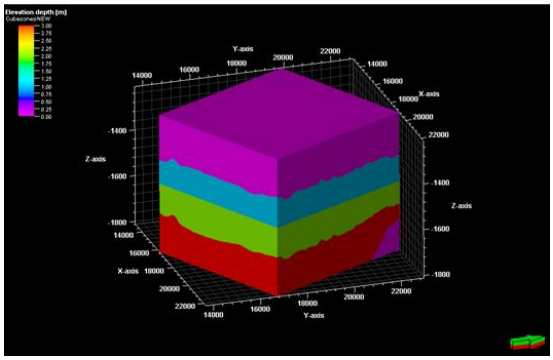

Figure 8 – Zones cube (Petrel view).

The creation of zone 0 is related to the necessity to introduce in the GSI zones algorithm a model with parallel boundaries. In this situation, it was necessary to create fictitious horizons that allowed to obtain a parallelism.

3. Calculation of GSI zones input parameters

The calculation of the input parameters included: i) the setting of AI local distributions for each defined zone, ii) the variography study for each defined zone, and iii) wavelet estimation.

i. Setting of AI local distributions

The setting of AI local distributions used available data from three wells. This allowed to get a global overview of the lithological behavior, and therefore, to create AI records and assign different types of facies for each zone. Thus the calculation of AI local distribution applied the Gassmann fluid substitution theory. The computation of Gassmann´s equations was performed using the Matlab2012 software, from which was possible to obtain AI value ranges for each type of facies, associated with different zones of the model.

The types of facies for each zone were defined as follows; zone 3 (seismic unit BA3) characterized by clays, zone 2 (seismic unit BA4 - "target" zone) composed of clays interbedded by thin sands, which corresponds to the turbidite channels system, and zone 1 (seismic unit BA5) correlated with clay and sandy clay facies.

The first step in the use of Gassmann equation consisted on the definition of input values. It was assumed that the "target" zone is at a depth of 2.000m (top of the reservoir). On this basis, it was possible to get the input values needed to compute the Gassmann equations (Table 2).

Table 2 - input values used to compute the Gassmann equations

Valores iniciais para as equações de Gassman	
VP	9.600 ft/s
VS	5.700 ft/s
Densidade	2.2 g/cm3
Temperatura	65 °C
Pressão	3.000 Psi
Sat. Inicial água	1.00

To simulate the AI values, for the two types of facies (sand and clay), it was necessary to establish the limits for petrophysical properties, in particular, clay percentages (VClay), effective porosity, final water saturation, and type of fluid present in the rock pores (brine or gas) (Table 3).

Table 3 - Petrophysical properties used to compute Gassmann equations

Modelo de Fácies (Parâmetros das equações de Gassman)		
Propriedade	Areias	Argilas
Porosidade	0.13 - 0.30	0 - 0.13
Volume Argila (% finos)	0 - 0.35	0.35 - 1.0
Saturação final água	0.1 - 0.6	0.6 - 1.0

The computation of Gassmann´s equations allowed to obtain AI intervals, which were correlated with types of facies in accordance to the simulated fluid (Table 4).

Table 4 - AI intervals obtain from Gassmann´s equations

Valores iniciais para as equações de Gassman	
Fácies e fluidos	Valores IA (kPa s/m)
Areias com Gás	4.600 - 5.600
Areias com Salmoura	5.500 - 6.500
Argilas com Salmoura	6.300 - 8.000

Based on AI intervals, it was possible to construct lithologic distributions that represent potential scenarios with different types of fluids present in rock pores. Being the "target" zone a lower lobe of the depositional "fan", it is expected that there is a higher volume of clay facies over the sands. In the present study, it was chosen to use triangular type distributions for each zone. The construction of the local distributions was performed using a geostatistical software, developed by CERENA (IST), Geoms2.

Exploratory data analysis characterized the univariate statistical behavior of the set samples. All possible information about the available data was extracted through the description and quantification of main statistical indicators.

This document only describes, in greater detail, the univariate analysis for both types of simulated fluids (brine and gas) present in the "target" zone.

i) Scenario A: "target" zone represented by clays and sand facies with brine.

In this scenario, for a total of 500 samples, the AI records a minimum value of 5.650kPa s/m and a maximum up to 7.982kPa s/m, the average value is 6.870kPa s/m, the median has a value of 6.900kPa s/m and a variance of 246.956 (Figure 9).

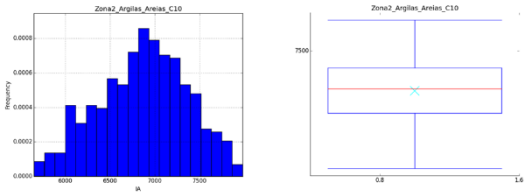

Figure 9 - Scenario A (brine) univariate analysis for the "target" zone

ii) Scenario B: "target" zone represented by clays and sand facies with gas.

In scenario B, were used 1.000 samples, the AI registers a minimum value of 4.608kPa s/m up to 7.956kPa s/m, the average value is 6.752kPa s/m, the median has a value of 6.839kPa s/m and variance of 399.884 (Figure 10).

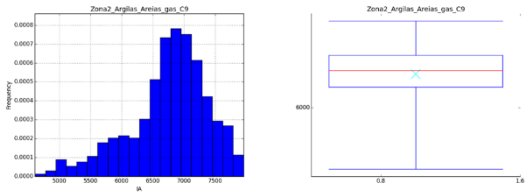

Figure 10 - Scenario B (gas) univariate analysis for the "target" zone

ii. Spatial continuity analysis

The theoretical models of variograms were used throughout the simulation and stochastic global inversion computation process. These variograms were also used to validate the obtained results, since the methods applied assume that the theoretical variograms, defined based on the experimental variograms, are always honored.

The study of the horizontal variography was performed based on spatial continuity analysis of seismic reflectors, through geostatistical Geoms software. For the calculation of experimental variograms was used Geovag module and for the adjustment of these variograms to theoretical variogram models the Geomod module. The definition of vertical continuity was performed considering the sedimentary basin geological study, in particularly, for units included in the model zones cube.

Theoretical variograms were all set with two structure models and there was no need to consider nugget effect. The threshold and amplitude were defined for each zone for main directions. The thresholds were defined considering total variance of the sample set. The amplitudes were defined in order to adjust

the theoretical models to experimental variograms. Likewise to the AI local distributions, only the theoretical variograms for main directions for "target" zone are presented (Figure 11).

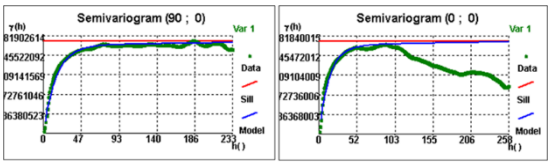

Figure 11 - Adjusted models of the variograms for the main directions of zone 2

iii. Wavelet estimation

The lack of well data in the area of the seismic data acquisition resulted in the inability to “tie” the data and estimate the wavelet, through time curve in well logging (checkshot), which allows to create a relationship between time-depth. Thus, the wavelet estimation used a statistical wavelet. The statistical wavelet, provided by CERENA team (IST), was extracted from seismic data using Hampson-Russell Suite software (CGG).

The length for the estimation of statistical wavelet was set at 121ms, which corresponds to 61 amplitude values.

The wavelet amplitude was scaled for each scenario, A and B, in order to obtain synthetic seismic amplitude values equivalent to those observed in real seismic data.

The statistical wavelet used for scenario A is represented in Figure 12.

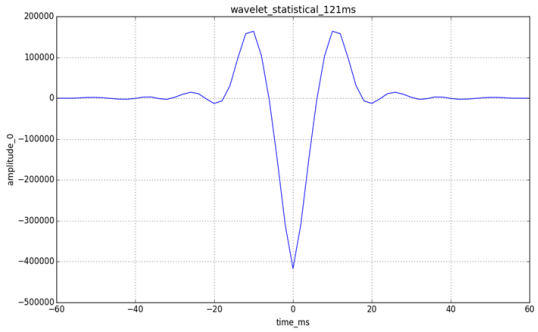

Figure 12 - Wavelet used for the scenario A, Geoms2 view

4. GSI zones algorithm results

The AI cubes resulted from the computation of GSI zones algorithm, for the two fluid scenarios, brine and gas, present in the "target" zone.

The differentiation of each scenario resulted in the preliminary assessment of AI local distribution, obtained by applying the Gassmann fluid replacement theory.

In this case study it was decided to compute GSI algorithm for 6 iterations with 32 realizations per iteration. The computation of the model zones, for scenario B, shows a high convergence between the synthetic and real seismic amplitudes (Figure 13). The same trend for the evolution of correlation was observed for scenario A.

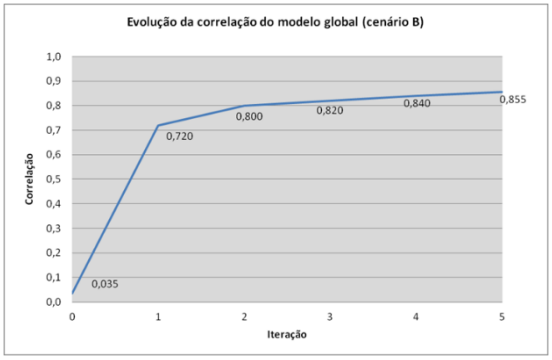

Figure 13 - Scenario B: Model zones evolution of the correlation for 6 iterations

Through experimentation with different numbers of realizations, it was establish that its

increase promotes a reduction in the standard deviation values. From a computational point of view, the execution of 32 realizations proved to be sufficient for this simulation.

- **Scenario A (simulated fluid: brine)**

The computation of the optimized input parameters allowed to obtain an overall correlation between the synthetic and real seismic amplitudes of 0.855 (Figure 14).

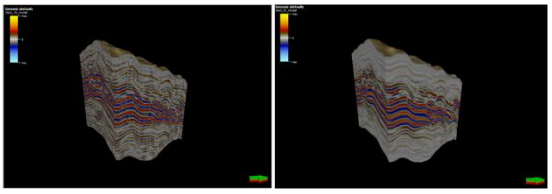

Figure 14 – Synthetic seismic cube (left) and real seimic cube (right)

The low dispersion of values around the xy axis reveals the high correlation value obtained between synthetic and real seismic models (Figure 15).

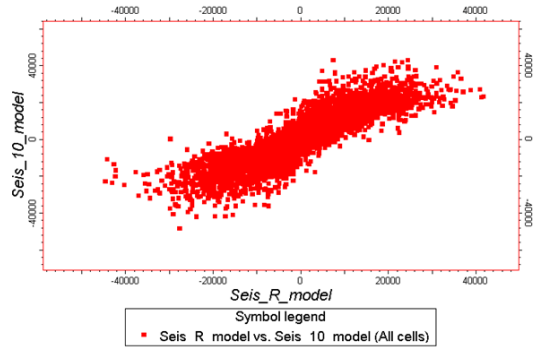

Figure 15 – Seismic amplitude correlation. Petrel output

The equivalence between the histograms confirms the high correlation obtained for scenario A (Figure 16).

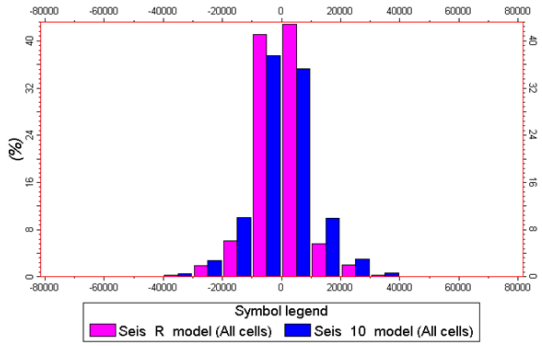

Figure 16 – Amplitude histograms for real seismic (purple) and synthetic seismic (blue)

In order to proceed with consistent analysis for the results obtained in GSI, for both scenarios, a position was defined in the model (*i = 125, j = 125, k = 193*). The selected position, for both scenarios, revealed the presence of clusters with low AI values and channels systems also observed in the real seismic cube.

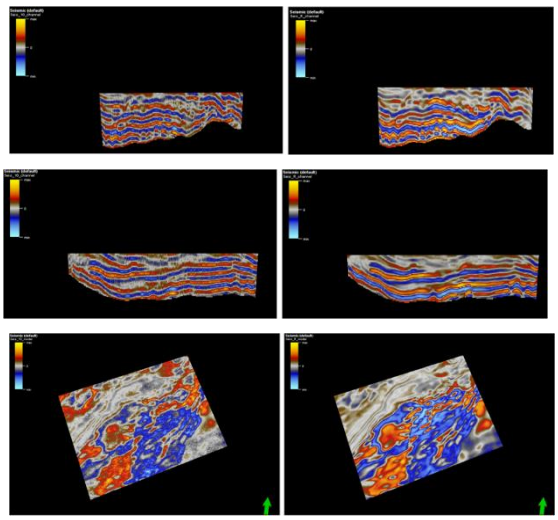

Figure 17 - Images obtained for synthetic seismic (left) and real (right) for the section defined by the position i = 125, j = k = 125 and 193, respectively

The images obtained of AI cube at the 6th iteration are presented below (Figure 18).

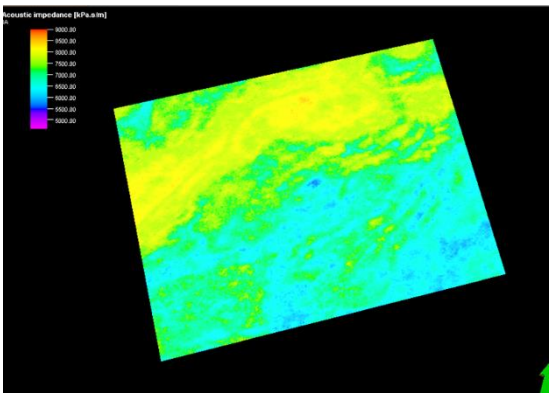

Figure 18 – AI cube for section defined by the position i = 125, j = 125 and k = 193, respectively

- **Scenario A (simulated fluid: gas)**

This scenario differs in the distribution of AI values and wavelet for the "target" zone. The statistical wavelet was scaled to minimize differences between real and synthetic amplitudes. The computation of the optimized parameters allowed to obtain an overall correlation between the synthetic and real seismic of 0.854 (Figure 19).

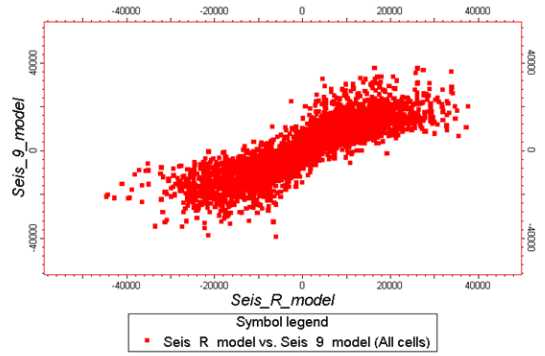

Figure 19 - Seismic amplitude correlation. Petrel output

Similarly to scenario A, it was noted that equivalence between the histograms confirms the high correlation obtained for scenario B (Figure 20).

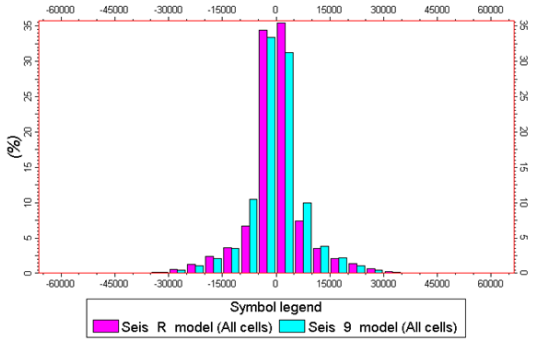

Figure 20 - Amplitude histograms for real seismic (purple) and synthetic seismic (blue).

The images obtained by AI cube at the 6th iteration are presented below (Figure 21).

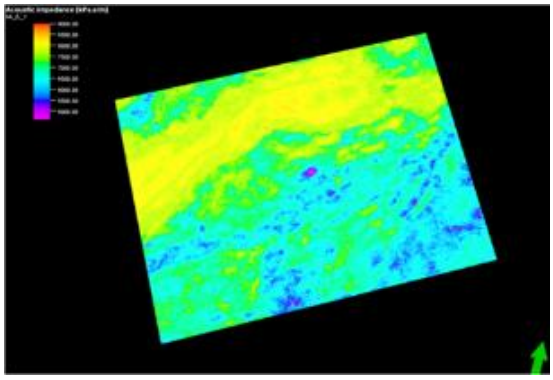

Figure 21 – AI cube for section defined by the position i = 125, j = 125 and k = 193, respectively

5. Conclusões

This study presents the theme of a subsampled field where the lack of information hinders the morphological characterization of potential hydrocarbons reservoir. The use of the GSI zones algorithm proved to be an additional and feasible tool in initial characterization phases, providing data with associated uncertainty evaluation for each simulated fluid scenario.

The use of Gassmann fluid substitution theory allowed to simulate different types of fluids present in the "target" zone, through ranges of AI values.

The input parameters of Gassmann equations, when well calibrated and comply with the conditions of pressure and temperature of the potential reservoir, proved to be a very consistent instrument.

The analysis performed for both scenarios allowed to identify a region (i = 125; j = 125 and k = 193) characterized by low AI values, well demarcated from the rest of the surrounding population. The identified region is associated with continuous seismic reflectors with very high negative amplitude, establishing the passage of a high AI environment to a lesser. This sharp contrast of amplitudes may suggest the presence of a sand body. Thus, this zone may have potential for storage hydrocarbons, because low impedance values are typically associated with high porosity values.

The proximity of the correlation values for each scenario (brine and gas) does not reveal about the presence of hydrocarbons, it only allows to identify confined areas characterized by low AI values, which can confirm the presence of sand bodies dating from the Miocene, as described in the geological study of the sedimentary basin of the study area.

The present study has the potential to be explored and deepened. The verification of the veracity of AI 3D models, obtained by GSI zones algorithm, for similar subsampled fields, may have considerable business advantages in the early stages of reservoir characterization, considering the huge investments required to conduct exploratory wells in remote regions, like deep-offshore fields.

The following steps in the use and confirmation of the robustness of the GSI zones algorithm may pass by calculating seismic attributes using the synthetic seismic cube (e.g.: RMS amplitude attribute), which can reinforce the presence of regions with low AI, identified by high RMS amplitude values.

6. References

Batzle, M. & Wang, Z. Seismic properties of pore fluids. Geophysics, 57, 11, pp. 1396-1408, 1992.

Bortoli, L., Alabert, F., & Journel, A. (1993). Constraining stochastic images to seismic data. Geostatistics (pp. 325-557). Troia'92: Kluwer, Dordrecht

Gassmann, F. Elastic waves through a oacking of spheres, Geophysics, 16, 673-685 pp, 1951.

Mavko G, Mukerji T & Dvorkin J. The Rock Physics Handbook, Cambridge University Press, 339 pp, 1998.

Nunes, R., Almeida, J. (2010). Paralelização dos Algoritmos Simulação Sequencial Gaussiana, Indicatriz e Direta. Computers & Geocienses Nº36.

Roque, A (2007). Tese de Doutoramento, Faculdade de Ciências - Universidade de Lisboa.

Soares, A., Diet, J. D., & Guerreiro, L. (2007). Stochastic Inversion with a Global Perturbation Method. Petroleum Geostatistics. Cascais, Portugal: EAGE.